

## Electrical Spin Transport in $n$ -Doped $\text{In}_{0.53}\text{Ga}_{0.47}\text{As}$ Channels

Youn Ho Park, Hyun Cheol Koo\*, Kyung Ho Kim, Hyung-jun Kim, and Suk Hee Han

Center for Spintronics Research, KIST, Seoul 130-650, Korea

(Received 1 December 2008, Received in final form 25 February 2009, Accepted 11 March 2009)

**Spin injection from a ferromagnet into an  $n$ -doped  $\text{In}_{0.53}\text{Ga}_{0.47}\text{As}$  channel was electrically detected by a ferromagnetic detector. At  $T = 20$  K, using non-local and local spin-valve measurements, a non-local signal of  $2 \mu\text{V}$  and a local spin valve signal of  $0.041\%$  were observed when the bias current was  $1$  mA. The band calculation and Shubnikov-de Haas oscillation measurement in a bulk channel showed that the gate controlled spin-orbit interaction was not large enough to control the spin precession but it could be a worthy candidate for a logic device using spin accumulation and diffusion.**

**Keywords :** InGaAs bulk channel, non-local measurement, local spin-valve measurement, electrical spin transport

### 1. Introduction

Conventional semiconductor devices are based on the control of electronic charge but recently the physical limitations have become obstacles to improvement of device performance. Spin transport device based on the manipulation of electron spin is one of the next generation devices drawing a great deal of attention as it potentially has higher performance through fast switching and non-volatile characteristics. A seminal device using spin transport is the spin field effect transistor (spin-FET) that utilizes spin injection, detection and the control of spin precession [1]. Recently, many studies have attempted to demonstrate spin transport from a ferromagnet (FM) into semiconductors [2, 3] and control of spin-orbit interactions as an essential parameter to control spin precession [4, 5].

In this paper, we executed non-local and local spin-valve measurement to confirm that a spin-polarized current was injected from the FM1 (injector) to an  $n$ -doped  $\text{In}_{0.53}\text{Ga}_{0.47}\text{As}$  channel, epitaxially grown by molecular-beam epitaxy, and injected spins was electrically detected by FM2 (detector). The effective magnetic field ( $B_{\text{eff}}$ ) was induced in the  $y$ -direction when the electrons move ( $k_x$ ) under a perpendicular electric field ( $E_z$ ) induced either internally or externally. The gate controlled spin-orbit interaction parameters were investigated by using the

Shubnikov-de Haas oscillation (SdH) measurement and the band structures are calculated with WinGreen simulator [6]. In the bulk channel, the vertical multilayer structure is very simple so that device application is very favorable. In this research, we report the spin-related phenomenon of  $n$ -doped  $\text{In}_{0.53}\text{Ga}_{0.47}\text{As}$  channels to investigate the feasibility of the device application.

### 2. Experimental

Fig. 1(a) shows the cross-sectional view of the substrate structure. The semiconductor channel was an  $n$ -doped  $\text{In}_{0.53}\text{Ga}_{0.47}\text{As}$  layer grown by molecular beam epitaxy on a semi-insulated InP(100) substrate. An  $\text{In}_{0.52}\text{Al}_{0.48}\text{As}$  buffer layer was deposited to release the mismatch between the  $\text{In}_{0.53}\text{Ga}_{0.47}\text{As}$  channel and the InP substrate. The thickness of the channel was  $40$  nm and  $4 \times 10^{18} \text{ cm}^{-3}$  of Si was  $n$ -doped in the channel to increase channel conductivity. The capping layer made of InAs was deposited to protect possible damage during the fabrication process. The carrier concentration and electron mobility of the channel were  $n_s = 4.98 \times 10^{18}$  ( $5.03 \times 10^{18}$ )  $\text{cm}^{-3}$  and  $\mu = 2,498$  ( $2,462$ )  $\text{cm}^2\text{V}^{-1}\text{s}^{-1}$  at  $1.8$  K ( $77$  K), respectively, obtained by the Hall measurement.

Two kinds of samples using an  $\text{In}_{0.53}\text{Ga}_{0.47}\text{As}$ -channel substrate were fabricated for the experiment. One sample was manufactured for the spin transport experiment which included spin injection and detection. This was a lateral spin-valve structure and a scanning electron micrograph is shown in Fig. 1(b). A channel width of  $8 \mu\text{m}$  was defined

\*Corresponding author: Tel: +82-2-958-5423  
Fax: +82-2-958-6851, e-mail: hckoo@kist.re.kr

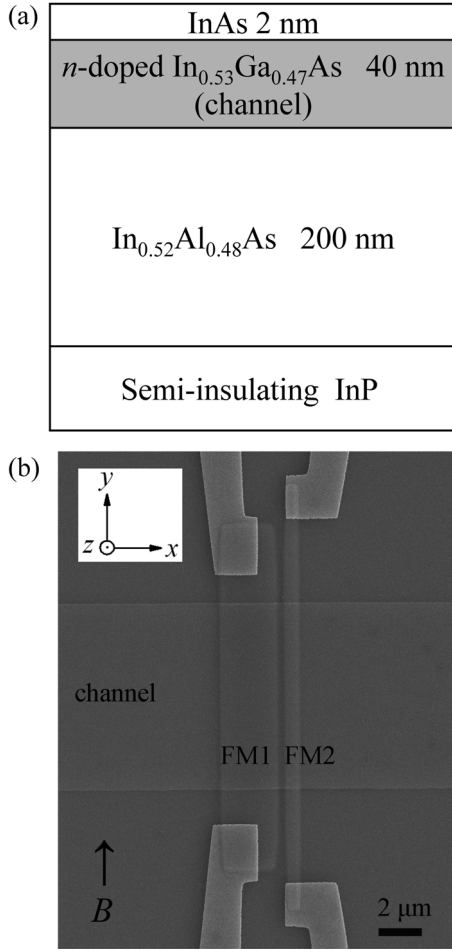


**Fig. 1.** (a) Cross-sectional view of  $n$ -doped  $\text{In}_{0.53}\text{Ga}_{0.47}\text{As}$  channel structure. (b) Scanning electron micrograph of a lateral spin valve device.

by using photolithography and ion milling. The  $\text{In}_{0.53}\text{Ga}_{0.47}\text{As}$  layer outside the channel was etched to a thickness of 50 nm from the top surface. No current flow in the outside area of the patterned channel was ensured. In this sample,  $\text{Ni}_{81}\text{Fe}_{19}$  was deposited using a sputtering system to form the two ferromagnetic electrodes (FMs). These FMs required different aspect ratios to achieve parallel and anti-parallel alignments with an external magnetic field. The thickness of the FMs was 80 nm and the lateral sizes were  $2.4 \mu\text{m} \times 17 \mu\text{m}$  (FM1) and  $0.4 \mu\text{m} \times 24 \mu\text{m}$  (FM2). The center-to-center distance between the FMs in this experiment was defined as the channel length of  $2.2 \mu\text{m}$ .

The other sample was made for the Hall and the Shubnikov-de Haas oscillation (SdH) measurements. A  $64 \mu\text{m}$ -wide channel was also defined by using photolithography and ion milling. The gate electrode was deposited on a 100 nm thick insulating layer made of  $\text{SiO}_2$  that electrically separated the Hall bar and gate electrode. A gate electrode was made of Ti/Au layer.

### 3. Results and Discussion

There are two different measurement geometries to electrically detect the injected spin-polarized electrons by using the magnetization correlation of the two FMs. The first type is a non-local measurement. In this measurement geometry, the spin-polarized current was diffused and detected by placing a ferromagnetic detector on the other side of the charge current [7]. Therefore, non-local measurement can minimize the unwanted effects such as a local Hall effects, anisotropic magnetoresistance and other extrinsic contributions [8]. Fig. 2(a) shows the non-local geometry (inset) and the measurement results at  $T = 20 \text{ K}$ . The spin-polarized current was injected into the  $\text{In}_{0.53}\text{Ga}_{0.47}\text{As}$  channel from the FM1. The electrical current flowed into the  $-x$ -direction but the charge current did not reach the detection FM. The accumulated spins at the interface of the ferromagnet-semiconductor were diffused in both directions and subsequently influenced the spin carrier concentration  $n_{\uparrow}$  and  $n_{\downarrow}$  in the channel. The total carrier concentration could be expressed as  $n_s = n_{\uparrow} + n_{\downarrow}$ . The external magnetic field was applied to the  $y$ -axis for

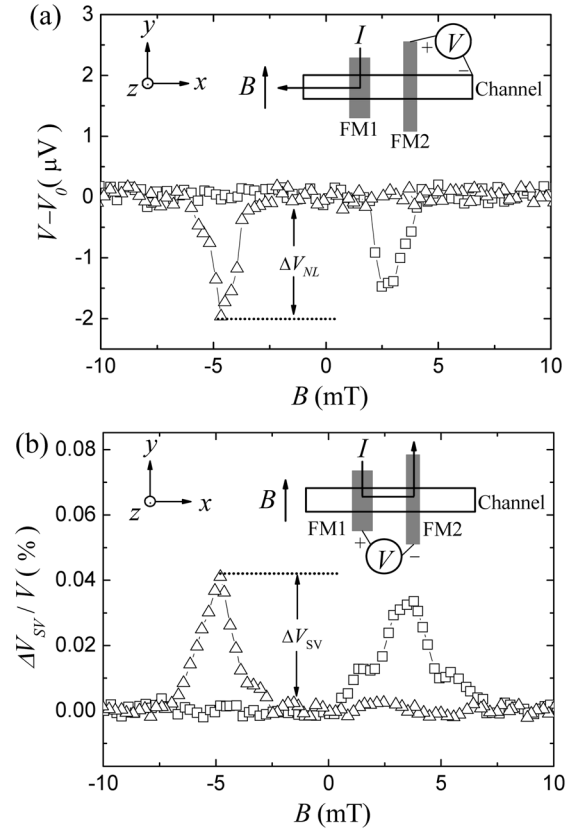


**Fig. 2.** Results of spin transport experiments at  $T = 20 \text{ K}$  and geometry of (a) non-local measurement and (b) local spin-valve measurement. The squares and triangles correspond to the field sweep up and down, respectively.

achieving the parallel and anti-parallel states of the FMs bearing different coercivities. In the field sweep-up process, the magnetization of both FMs was initially saturated to the  $-y$ -direction (spin-down state). In this state the spin-down was injected from the FM1 causing the spin-down distribution ( $n_{\downarrow}/n_s$ ) in the channel to increase and raise the Fermi level of spin-down chemical potential. In this case, the detector (FM2) was parallel to injector (FM1), thus the detector read the spin-down chemical potential, which is at a high potential status. Since the coercivity of the FM1 was smaller than the FM2, the magnetization of FM1 was first realigned to the  $+y$ -direction with an increasing external magnetic field. At this moment, the spin-up distribution probability ( $n_{\uparrow}/n_s$ ) increased in the channel. In this state, the Fermi level of spin-up chemical potential of the FM2 was aligned to the Fermi level of the spin-up (minor spin) chemical potential of the channel, thus the low potential state was measured. As magnetic field was increased, the magnetization of the FMs returned to the parallel alignment. Therefore, the potential difference between the parallel and antiparallel states was observed in the non-local method. The detected signal ( $\Delta V_{NL}$ ) was  $2 \mu\text{V}$  and the current bias was  $1 \text{ mA}$ .

The second type was a local spin-valve measurement. When the current was injected from FM1 and FM2, the voltage was measured at the same nodes as shown in the inset of Fig. 2(b) [3, 9]. This measurement allowed measurement of the spin-dependent resistance change at the interface. In this geometry, there were also two levels of the detected voltage that depended on the magnetization alignment of the FMs. Fig. 2(b) shows the local spin-valve measurement results at  $T = 20 \text{ K}$ . The detected signal ( $\Delta V_{SV}/V$ ) was  $0.041\%$  and the bias current was  $1 \text{ mA}$ .

Next, the possibility of controlling the spin-orbit interaction strength of the channel by the gate electrode was considered. The conduction band potential and the carrier concentration were calculated with applying the gate voltage in the  $z$ -direction as shown in Fig. 3. The WinGreen simulator was utilized, with its data files for the band calculation [6]. The spin-orbit interaction parameter,  $\alpha$ , depended on the electric field,  $E$ , inside the channel [4]. The electric field was proportional to the potential gradient. From the calculation results, the magnitude of the potential gradient in the channel was found to increase with increasing negative gate voltage. The carrier distribution was also decided by the potential gradient. The spin-splitting energy ( $\Delta_S$ ) was expressed as  $\Delta_S = 2k_F\alpha$ , where the Fermi wave number  $k_F$  equals  $(3\pi^2n_s)^{1/3}$ . The carrier concentration  $n_s$  can be obtained from the Hall or SdH measurements. Fig. 4(a) shows the carrier concentration  $n_s$  and mobility  $\mu$  dependence on the gate voltages

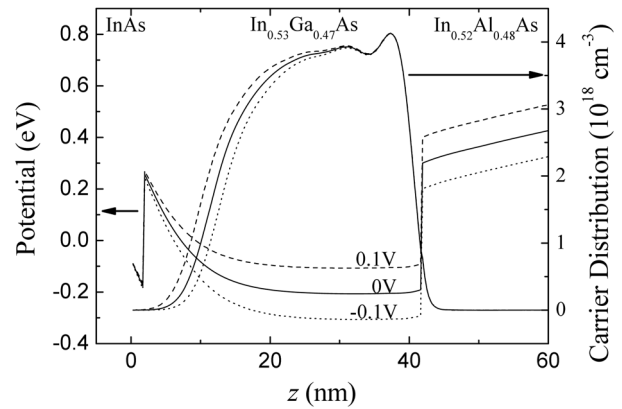


**Fig. 3.** Energy band diagram and charge distribution of  $n$ -doped  $\text{In}_{0.53}\text{Ga}_{0.47}\text{As}$  channel for various gate voltages. The  $z$  is the distance from the top surface.

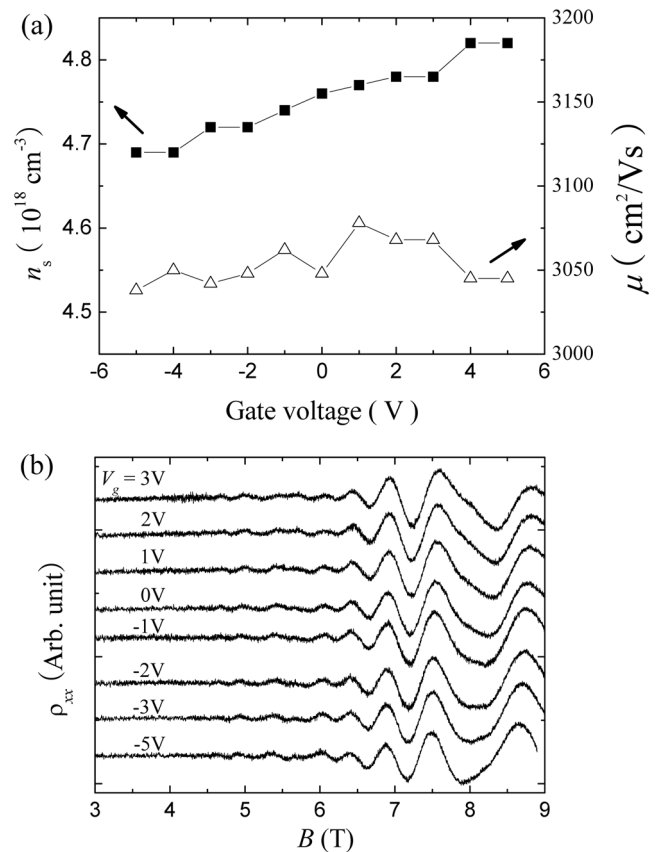


**Fig. 4.** Gate voltage dependence of the Hall and Shubnikov-de Haas oscillation measurements (a) Carrier concentration and electron mobility as a function of gate voltages. The squares and triangles correspond to the total carrier concentration ( $n_s$ ) and mobility ( $\mu$ ), respectively. (b) Results of SdH measurements with gate voltages at  $T = 1.8 \text{ K}$ .

at  $T = 1.8 \text{ K}$ . These results indicate that  $n_s$  and  $\mu$  are not changeable in the varying gate voltages. Fig. 4(b) shows the measured signals of the SdH oscillation at  $T = 1.8 \text{ K}$ .

In the measurement, the current bias was  $5 \mu\text{A}$  and the channel resistance ( $\rho_{xx}$ ) was measured with increasing the magnetic field perpendicular to the plane at various gate voltages. Spin-up and -down electrons generate different oscillation frequencies and beat patterns appear when these frequencies are synchronized. A period of the beat patterns is proportional to the spin splitting energy [5]. Two node positions in the beat patterns are required to estimate the spin-orbit interaction parameter. From our results, however, clear beat patterns were not observed, even with the external gate voltages. The possible reasons why the beat pattern does not occur are thus considered. Firstly, at zero voltage the carrier distribution was relatively broad so that the internal electric field from the charge asymmetry was negligible. When the gate voltage was applied, charge distribution asymmetry occurs, but the reasonable range of gate voltage was not enough to induce Rashba effect. A gate voltage of 0.1 V in Fig. 3 was actually a very large value, because almost all voltage drop occurred within the gate oxide. To apply 0.1 V to the channel, a tremendous external gate voltage is necessary. The structure-induced electric field of the bulk channel is small in comparison with a two dimensional electron gas (2DEG) system bearing an interfacial electric field arising from asymmetry of the potential well even without the external electric field. Therefore the bulk channel can be potentially used for a logic device that utilizes spin accumulation and spin diffusion [10] instead of a spin-orbit interaction induced switching device.

#### 4. Conclusions

In conclusion, we observed clear evidence of spin transport in an  $\text{In}_{0.53}\text{Ga}_{0.47}\text{As}$  bulk channel using a lateral spin valve device. The injected spins from a ferromagnet were transported and detected at the other ferromagnet in the non-local and local spin-valve measurement. The band calculation and Shubnikov-de Haas oscillation measure-

ments for our structure indicate that the electric field induced to the channel was changed by an external gate voltage but the amount of band bending was not large enough to control the spin-orbit interaction. Since spin diffusion length is usually inversely proportional to the spin-orbit interaction strength, a long spin diffusion length is expected in the  $n$ -doped InGaAs bulk channel. In addition, the vertical structure of the bulk channel is very simple so that the bulk-channel-based spin device can be utilized for high efficiency spin transport devices.

#### Acknowledgment

This work was supported by the KIST Institutional Program.

#### References

- [1] S. Datta and B. Das, *Appl. Phys. Lett.* **56**, 655 (1990).
- [2] X. Lou, C. Adelman, S. A. Crooker, E. S. Garlid, J. Zhang, K. S. M. Reddy, S. D. Flexner, C. J. Palmström, and P. A. Crowell, *Nature Physics*. **3**, 197-202 (2007).
- [3] H. C. Koo, H. Yi, J.-B. Ko, J. Chang, S.-H. Han, D. Jung, S.-G. Huh, and J. Eom, *Appl. Phys. Lett.* **90**, 022101 (2007).
- [4] J. Nitta, T. Akazaki, and H. Takayanagi, *Phys. Rev. Lett.* **78**, 1335 (1997).
- [5] J. H. Kwon, H. C. Koo, J. Chang, and S.-H Han, *Appl. Phys. Lett.* **90**, 112505 (2007).
- [6] K. M. Indlekofer and J. Malindretos, WinGreen-Simulation, Forschungszentrum Jülich GmbH, Germany (2004).
- [7] B. C. Lee, *J. Magnetism* **13**, 81 (2008).
- [8] D. D. Awschalom, D. Loss, and N. Samarth, *Semiconductor Spintronics and Quantum Computation*, Springer-Verlag, Berlin (2002) pp. 31-87.
- [9] J. Ku, J. Chang, H. Koo, J. Eom, S.-H Han and G. Kim, *J. Magnetism* **12**, 152 (2007).
- [10] D. Dery, P. Dalal, Ł. Cywiński and L. J. Sham. *Nature* **447**, 573 (2007).